

# Relation of the stress state in the contact zone and the forces acting in the roller mechanisms

*Gulomjon Yakubov\**, *Janna Dalakyan*, *Sayyora Atadjanova*, and *Sarvar Tashpulatov*

Tashkent University of Architecture and Civil Engineering, Tashkent, Uzbekistan

**Abstract.** Mathematical models were developed to study the distribution pattern of shear and friction stresses in the roll contact zone. These models establish a relationship between the stress state in the contact zone, the forces acting on the roller mechanisms, and the shape of the roll contact curve in driven and free rollers. The distribution of normal stresses determines the distribution of shear stresses along the contact curve, the compliance of the material strip and the roller coating, and the forces acting on the roller mechanism.

## 1 Introduction

Technological processes in roller mechanisms are made possible by forces between the material being processed and the roller coatings. The contact stresses in the contact zone of the rollers are the direct characteristics of the intensity of these forces.

Following the main function performed, all roller mechanisms present pulling, compressing, and guiding devices. Depending on the function performed (pulling, compressing, or guiding) and the nature of the interaction, different types of contact stresses arise in the contact zone of the rolls [1]. For pulling and compressing roller mechanisms, fields of shear and normal stresses arise on the contact surface of the rollers with the material being processed. The main stress field in pulling mechanisms is normal stress, while in compressive mechanisms, it is shearing stress. For guiding mechanisms, the main stress field is the reaction force of the roller caused by the tension of the incident and descending branches.

A quantitative measure of contact stresses is the so-called friction stress models; function  $f(\alpha)$ , connecting shear  $t(\alpha)$  and normal  $n(\alpha)$  stresses is obtained by the following formula:

$$f(\alpha) = \frac{t(\alpha)}{n(\alpha)}, \quad (1)$$

where  $\alpha$  – is the polar angle.

References [5-15] are devoted to the development of friction stress models in metal rolling. However, the currently developed models of friction stress in metal rolling do not provide high accuracy and reliability in predicting the parameters of roller mechanisms [16].

In roller mechanisms, when the rollers are covered with an elastic coating, the contact interaction of the strip and the coating of the rollers occurs along the roll contact curves. Here

---

\* Corresponding author: [shavkat-xurramov59@mail.ru](mailto:shavkat-xurramov59@mail.ru)

the distribution pattern of contact stresses depends on the shape of the roll contact curves [17-18].

Research conducted in [19-27] is devoted to the distribution of contact stresses in the roller mechanisms of technological machines. However, these publications do not consider the impact of forces acting in the roller mechanisms and the shape of the roll contact curves on the stress state in the roll contact zone.

This article analyzes the impact of forces acting on roller mechanisms and the shape of roll contact curves on friction stress models.

## 2 Materials and methods

Let us consider a symmetrical roller mechanism, where both rollers are driven. Then, in a steady-state process, each roller is affected by the pressure force of the gripping device  $Q$ , the reaction of the roll supports  $F$ , the moment of resistance  $M$ , and elementary normal  $dN$  and shear  $dT$  forces (Figure 1).

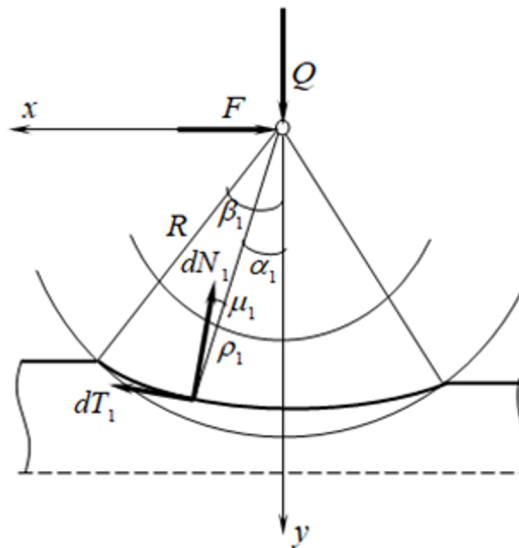


**Fig. 1.** Diagram of forces acting on the roller.

Consider the elementary forces in the compression and recovery zones separately. From the equilibrium condition of the roller in the compression zone, we obtain:

$$-F_1 + T_{1x} + N_{1x} = 0, \quad Q_1 + T_{1y} + N_{1y} = 0$$

or

$$dF_1 = T_{1x} + N_{1x}, \quad dQ_1 = -T_{1y} - N_{1y} = 0.$$

From the diagram of forces (Figure 1), we obtain

$$dF_1 = dT_1 \cos(\alpha_1 - \beta_1) - dN_1 \sin(\alpha_1 - \beta_1), \tag{2}$$

$$dQ_1 = dT_1 \sin(\alpha_1 - \beta_1) + dN_1 \cos(\alpha_1 - \beta_1), \tag{3}$$

where  $\rho_1, \alpha_1$  – are the polar coordinates of the points of the compression zone,  $\beta_1$  – is the angle between force  $dN_1$  and radius  $\rho_1$ , determined by the following formula [28]

$$\operatorname{tg} \beta_1 = \frac{\rho_1'}{\rho_1}. \quad (4)$$

### 3 Results and discussion

From equality (2) and (3), we determine:

$$\frac{dF_1}{dQ_1} = \frac{dT_1 \cos(\alpha_1 - \beta_1) - dN_1 \sin(\alpha_1 - \beta_1)}{dT_1 \sin(\alpha_1 - \beta_1) + dN_1 \cos(\alpha_1 - \beta_1)} \quad (5)$$

or

$$\frac{dF_1}{dQ_1} = \frac{dT_1 - dN_1 \operatorname{tg}(\alpha_1 - \beta_1)}{dT_1 \operatorname{tg}(\alpha_1 - \beta_1) + dN_1}. \quad (6)$$

In a steady-state process  $\frac{F_1}{Q_1} = k_1 = \text{const}$  [19]. It follows that  $\frac{dF_1}{dQ_1} = k_1$ .

Let  $k_1 = \operatorname{tg} \gamma_1$ . Then from equality (4), we obtain

$$\operatorname{tg} \gamma_1 = \frac{dT_1 - dN_1 \operatorname{tg}(\alpha_1 - \beta_1)}{dT_1 \operatorname{tg}(\alpha_1 - \beta_1) + dN_1}. \quad (7)$$

Transforming equalities (7), we find

$$\frac{dT_1}{dN_1} = \operatorname{tg}(\alpha - \beta + \gamma). \quad (8)$$

The modules of normal and shear forces are expressed as:

$$dN_1 = n_1 dl_1, \quad dT_1 = t_1 dl_1, \quad (9)$$

where  $n_1, t_1$  – are the normal and shear stresses distributed in the compression zone,  $dl_1$  – is the elementary arc of the compression zone.

Substituting expressions (9) into equalities (8), we obtain:

$$\frac{t_1}{n_1} = \operatorname{tg}(\alpha_1 - \beta_1 + \gamma_1), \quad -\mu_1 \leq \alpha_1 \leq 0, \quad (10)$$

$\mu_1$  – is the angle of nip.

It is known [23] that

$$R \frac{\cos \mu_1}{\cos \alpha_1} \leq \rho_1 \leq R. \quad (11)$$

Considering equality (10) and inequality (11), we obtain  $0 \leq \operatorname{tg} \beta_1 \leq \operatorname{tg} \alpha_1$  or  $0 \leq \beta_1 \leq \alpha_1$ .

From the last equality, it follows that  $\alpha_1 - \beta_1 = m_1 \alpha_1$ , where  $0 \leq m_1 \leq 1$ . Here,  $m_1 = 0$  for  $\rho_1 = R \frac{\cos \mu_1}{\cos \alpha_1}$ ;  $m_1 = 1$  for  $\rho_1 = R$ . We can say that  $m_1$  determines the compliance

of the strip of material and the roller coating in the contact zone of the roller mechanism, and, therefore, we can call it the compliance ratio.

Then from equality (10), we obtain:

$$\frac{t_1}{n_1} = \operatorname{tg}(m_1 \alpha_1 + \gamma_1)$$

or in the first approximation

$$\frac{t_1}{n_1} = m_1 \operatorname{tg} \alpha_1 + \operatorname{tg} \gamma_1, \quad -\mu_1 \leq \alpha_1 \leq 0, \quad (12)$$

since  $m_1 \alpha_1 < 1$ .

By analogy with (12), we find the values for the recovery zone:

$$\frac{t_2}{n_2} = m_2 \operatorname{tg} \alpha_2 + \operatorname{tg} \gamma_2, \quad 0 \leq \alpha_2 \leq \mu_2, \quad (13)$$

where  $\operatorname{tg} \gamma_2 = \frac{F_2}{Q_2}$ .

Generalizing equalities (12) and (13), we obtain:

$$\frac{t(\alpha)}{n(\alpha)} = \begin{cases} m_1 \operatorname{tg} \alpha_1 + \operatorname{tg} \gamma_1, & -\mu_1 \leq \alpha \leq 0, \\ m_2 \operatorname{tg} \alpha_2 + \operatorname{tg} \gamma_2, & 0 \leq \alpha \leq \mu_2. \end{cases} \quad (14)$$

Note that  $\alpha_1 = \alpha_2 = 0$ ,  $t_1(0) = t_2(0)$ ,  $n_1(0) = n_2(0)$ . Considering this condition, we have

$$\operatorname{tg} \gamma_1 = \operatorname{tg} \gamma_2 = \operatorname{tg} \gamma = \frac{F}{Q}.$$

Then from system (14), we obtain

$$t(\alpha) = n(\alpha) \begin{cases} \frac{F}{Q} + m_1 \operatorname{tg} \alpha_1, & -\mu_1 \leq \alpha \leq 0, \\ \frac{F}{Q} + m_2 \operatorname{tg} \alpha_2, & 0 \leq \alpha \leq \mu_2. \end{cases} \quad (15)$$

System (15) analyzes the relationship between contact stresses distributed along the roll contact curve and the forces acting in the roller mechanism when the rollers are driven. It also determines the impact of the shape of the roll contact curve on the stress state in the roller mechanism.

When a roller is free, the forces  $T$  and  $F$  acting on it, change direction. Then, from the system, we determine:

$$t(\alpha) = -n(\alpha) \begin{cases} -\frac{F}{Q} + m_1 \operatorname{tg} \alpha_1, & -\mu_1 \leq \alpha \leq 0, \\ -\frac{F}{Q} + m_2 \operatorname{tg} \alpha_2, & 0 \leq \alpha \leq \mu_2. \end{cases} \quad (16)$$

From systems (15) and (16), it follows that the distribution of shear stresses along the roll contact curve is affected by the distribution of normal forces, the forces acting on the roller, the shape of the roll contact curve, and the method of kinematic coupling.

Considering systems (15) and (16) and equality (1), we determine the friction stress model for a drive roller

$$f(\alpha) = \begin{cases} \frac{F}{Q} + m_1 \operatorname{tg} \alpha_1, & -\mu_1 \leq \alpha \leq 0, \\ \frac{F}{Q} + m_2 \operatorname{tg} \alpha_2, & 0 \leq \alpha \leq \mu_2. \end{cases} \quad (17)$$

For a free roller

$$f(\alpha) = \begin{cases} \frac{F}{Q} - m_1 \operatorname{tg} \alpha_1, & -\mu_1 \leq \alpha \leq 0, \\ \frac{F}{Q} - m_2 \operatorname{tg} \alpha_2, & 0 \leq \alpha \leq \mu_2. \end{cases} \quad (18)$$

From system (17), it follows that the ratio of contact stresses in the contact zone of the rollers is not constant, but changes at each point of the contact zone; therefore, we can say that in the contact zone of the roller mechanisms, Amonton's law is not observed.

We performed calculations of the ratio of contact stresses in the drive roller when force  $F$  varied within the following limits  $-0.2Q \div 0.2Q$ . The calculation results shown in Figure 2 are consistent with the results of other studies [12, 15].

The influence of the compliance of the roller coating and the strip of material on the ratio of contact stresses was studied by comparing their graphs when  $m$  ( $m = m_1 = m_2$ ) varied within the limits  $0.2 \div 1.0$  (Figure 3).

To study the impact of kinematic coupling on the ratio of contact stresses, calculations were conducted using systems (17) and (18). Figures 3 and 4 show the results of calculations for  $F = 0.6Q$  for various values of  $m_1$ : 1–0.2, 2–0.6, 3–1.0.

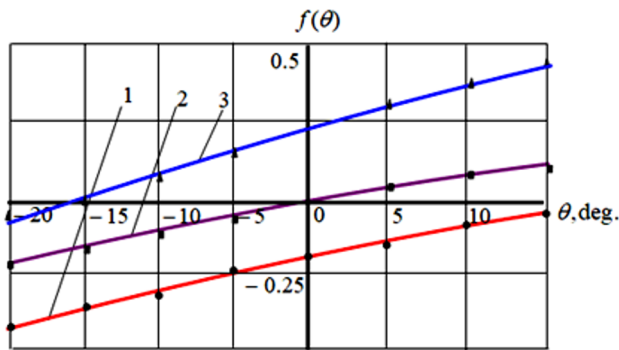


**Fig. 2.** The influence of external forces acting on the rollers on the ratio of contact stresses in the drive roller at  $m = 0.6$ : 1– $F = -0.2Q$ , 2– $F = 0$ , 3– $F = 0.2Q$ .

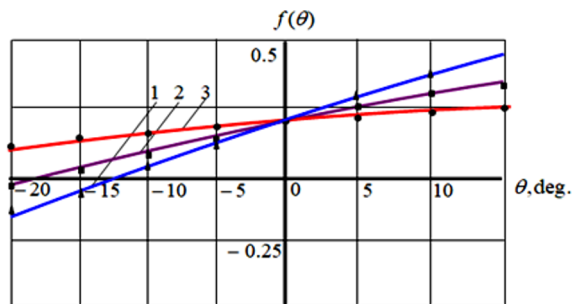


**Fig. 3.** The impact of the compliance of the roller coating and the strip of material on the ratio of contact stresses in the drive roller at  $F = 0.2Q$ : 1– $m = 0.2$ , 2– $m = 0.6$ , 3– $m = 1.0$ .

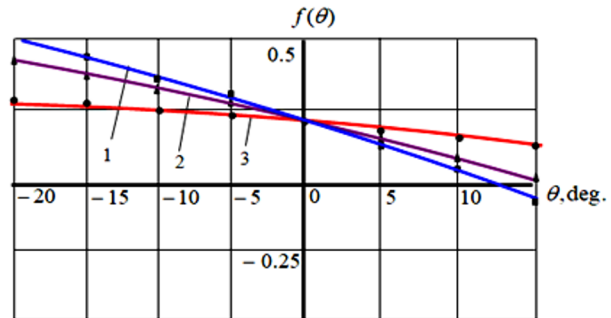


**Fig. 4.** The influence of the compliance of the roller coating and the strip of material on the ratio of contact stresses in the free roller at  $F = 0.2Q$ :  $1 - m = 0,2$ ,  $2 - m = 0,6$ ,  $3 - m = 1,0$ .

## 4 Conclusion

Mathematical models of the distribution patterns of shear and friction stresses in the roll contact zone were developed.

The models relate the stress state in the contact zone with the forces acting in the roller mechanisms and the shape of the roll contact curve when the roller is driven or free.

The distribution pattern of shear stresses along the contact curve is characterized by the distribution of normal stresses, the compliance of the strip of material and roller coating, and the forces acting on the roller mechanism.

## References

1. A.A. Smolentsev, D.N. Chekischev, J Modeling and development of metal forming processes **2**(29) (2019)
2. Ya.D. Vasiliev, R.A. Zamogilny, A.Yu.Kovtun, J. Metal forming **1**(46) (2018)
3. V.A. Nikolaev, J. Rolling production **9** (2013)
4. V.A. Haritonov, J. Blauk productions in mech.eng. **7** (2013)
5. V.A. Sinitskiy, Yu.L. Rybakov, J. Rolled products production **8** (2004)
6. S.I. Platov, P.P. Dema, R.N. Amirov, J. Rolled products production **9** (2012)
7. G.A. Baranov, J. Steel. **6** (2014)
8. A.L.Voronsov, Yu.Ch. Khatsiev, J. Engineering magazine with appendix 2014 **59** (2014)
9. S.V. Belyaev, J. Scientific life **4** (2018)
10. I.K. Oginskiy, J. Metal and casting of Ukraine **1** (2011)
11. V.M. Chuveyko, Bulletin of the Don State Tech.Univ. **12** (2012)
12. Ya.D. Vasiliev, M.I. Zamogilny, A.Yu. Kovtun, R.A. Zamogilny. J. Metal forming. **3**(36) (2013)
13. Sh.R. Khurramov, F.Z. Kurbanova, AIP Conference Proceedings **2637** 060004 (2022). <https://doi.org/10.1063/5.0118674>

14. Sh.R. Khurramov, B. Abduraxmanov, AIP Conference Proceedings **2637** 060003 (2022). <https://doi.org/10.1063/5.0118673>
15. Sh.R. Khurramov, F.S. Khalturaev, F.Z. Kurbanova, J. Izv.Vyss. Ucheb. Zav. Tech. Tekstil. Prom **4(394)** (2021)
16. A. Amanov, Sh.R. Khurramov, G.A. Bahadirov, A. Abdukarimov, T.Yu. Amanov, Journal of Leather Science and Engineering **3(14)** (2021)
17. Sh.R. Khurramov, F.S. Khalturaev, F.Z. Kurbanova, Design and Application for Industry 4.0. Studies in Systems, Decision and Control **342** (2021)
18. X. Akromov et al., J. AIP Conf.Proc. **2467** 060020 (2022)
19. M.U. Musirov, E.S. Buriev, Journal of Physics Conf.Series. **1889** 042020, (2021)
20. N.U. Annaev et.al., Journal of Physics Conf. Series. **2969** 060036 (2024)
21. Sh.R. Khurramov, F.S. Khalturaev, F.Z.Kurbanova, Journal of Physics Conf. Series. **2373** 072002 (2023). <https://www.doi.org/10.1088/1742-6596/2373/072002>
22. A. Rasulev et al., Journal of Physics Conf.Series. **1889** 042032 (2021)
23. D. Sulaymanova et al., E3S Web of conf. **443** 03006 (2023)
24. Sh.R. Khurramov, G.A. Bahadirov, A. Abdukarimov, J. Izv.Vyss. Ucheb. Zav. Tech. Tekstil. Prom **1(397)** (2022)
25. Sh.R. Khurramov, F.S. Khalturaev, F.Z. Kurbanova, E3S Web of Conf. **376** 01053 (2023). <https://doi.org/10.1051/e3sconf/20283760153>